Saturation Transfer Difference Measurements with SU(VAR)3−9 and *S*-adenosyl-L-methionine†

Karsten Seeger,‡ Sandro Lein,§ Gunter Reuter,§ and Stefan Berger*,‡

Institute of Analytical Chemistry, University of Leipzig, Johannisallee 29, D-04103 Leipzig, Germany, and Institute of Genetics, Biologicum, Martin Luther University Halle, Weinbergweg 10, D-06120 Halle (Saale), Germany

Received October 21, 2004; Revised Manuscript Received February 5, 2005

ABSTRACT: Saturation transfer difference NMR measurements were performed to investigate the interaction of *S*-adenosyl-L-methionine (AdoMet) with SU(VAR)3−9 from *Drosophila melanogaster*. SU(VAR)3−9 has a SET domain and plays an important role in methylation of lysine-9 of histone H3 which results in gene silencing. We determined the binding epitope of AdoMet and compared it with a crystal structure of another SET protein.

The methyl donor for most methylation reactions is *S*-adenosyl-L-methionine (AdoMet)[1], which is converted to *S*-adenosyl-L-homocysteine. The methyl group can be transferred not only to small molecules, for example, lipids and vitamin B_{12} (*1*), but also to macromolecules such as DNA or proteins (for a mechanistic consideration/review see ref *2*).

Methylation of lysine residues of histones (DNA binding proteins) plays a main role in chromatin regulation and marks functionally distinct chromatin regions (*3*, *4*). The reaction, catalyzed by histone methyltransferases, results either in activation or repression of gene transcription (*5*). Methylation of lysine-9 of histone H3 as a repressive mark leads to gene silencing caused by the formation of heterochromatic structures, catalyzed by SU(VAR)3−9 from *Drosophila melanogaster* (*6*, *7*), Clr4 from fission yeast (*8*), and DIM-5 from *Neurospora crassa* (*9*). DIM-5 and Clr4 have a structural and functional homology to SU(VAR)3−9. Methylation of lysine-4 results in activation of transcription due to formation of euchromatin (e.g., SET7/9). The highly conserved SET domain is the central part for catalyzing the reactions (*7*, *10*, *11*).

Until now, no structure of SU(VAR)3−9 was known. There are several crystal structures of methyltransferases with a SET domain that have been published, human SET7/9 (*12*−*15*), DIM-5 (*16*), pea Rubisco large subunit methyltransferase (*17*), and Clr4 (*18*). A structure with the cofactor AdoMet is only known for SET7/9 (*13*); all other structures contain the cofactor product AdoHcy.

The differences in the number of methyl groups which are transferred to the ϵ-amino group of lysine can be derived from the crystal structures. Nevertheless, it would be very interesting to characterize the interaction between a SET protein, catalyzing the methylation of lysine-9, and the cofactor in solution.

We therefore wanted to determine the binding epitope of AdoMet in order to get some insight into the interaction with SU(VAR)3−9. Saturation transfer difference NMR seemed to be an appropriate method (*19*, *20*, *21*).

MATERIALS AND METHODS

SU(VAR)3−9 (residues 218−635) was expressed as glutathione-*S*-transferase fusion protein in pGEX 6P1 in *Escherichia coli* BL21 pLys and purified on glutathione-*S*-sepharose (Amersham). The GST tag was removed by overnight treatment with PreScission Protease (Amersham) before ultrafiltration and D_2O exchange with Amicon Ultra centrifugal filter devices (Millipore). The samples of SU(VAR)3−9 and SU(VAR)3−9*GST were prepared in 1× PBS (140 mM NaCl, 2.7 mM KCl, 10 mM Na_2HPO_4, and 1.8 mM KH_2PO_4) and 2× PBS, pH* 7.8, in D_2O, respectively.

S-Adenosyl-L-methionine was purchased from Sigma (A 7007) and first used without further purification, despite a purity of only 70%, where the main contaminant is, according to NMR spectroscopy, the (+)-diastereomer; the concentrations given are not corrected. We wanted to test the capability of STD-NMR and the binding behavior of SU(VAR)3−9, because the other impurities are likely decomposition products of AdoMet. In preliminary experiments, we found a presumable interaction of SU(VAR)3−9 and *p*-toluolsulfonic acid present in the AdoMet preparation, and therefore, we used the chloride salt of AdoMet. On the request of a referee, we have purified the AdoMet material according to the procedure given by ref *22* using adsorption on IRC-50 ion exchange (Aldrich), elution with 0.1 N HCl, and reabsorption on XAD-7 ion exchange (Aldrich) and elution

† This work was supported by the Deutsche Forschungsgemeinschaft, SFB-610 "Variation in Protein Conformation: Cell Biological and Pathological Relevance", Projects A2 and A7.

* Corresponding author. E-mail, stberger@rz.uni-leipzig.de; phone, +49-341-97-36101; fax, +49-341-97-36115.

‡ University of Leipzig.

§ Institute of Genetics.

[1] Abbreviations: AdoHcy, *S*-adenosyl-L-homocysteine; AdoMet, *S*-adenosyl-L-methionine; COSY, correlation spectroscopy; DSS, 4,4-dimethyl-4-silapentane-5-sulfonic acid sodium salt; GST, glutathion-*S*-transferase; HSQC, heteronuclear single quantum correlation; HMT, histone methyltransferase; NOESY, nuclear Overhauser effect spectroscopy; PBS, phosphate buffered saline; pH*, pH-meter reading; SET, SU(VAR)3−9, Enhancer of zeste, Trithorax; STD, saturation transfer difference; SU(VAR), Suppressor of variegation.

10.1021/bi047749x CCC: $30.25 © 2005 American Chemical Society
Published on Web 03/29/2005

with 0.1 N HCl. All relevant spectra have been taken again with this purified material and freshly expressed SU(VAR)3−9 giving essentially the same results. It should be mentioned that the (+)-diastereomer of AdoMet cannot be removed by this procedure and that AdoMet even epimerizes spontaneously (*23*). The well-separated methyl group signal of the (+)-diastereomer, however, does not yield an STD effect, and thus, it can be safely assumed that this (+)-diastereomer is not involved in binding.

All NMR measurements were performed on a Bruker Avance 700 spectrometer with a 5 mm inverse triple-resonance probehead and a 300 W proton amplifier. The spectra were recorded with TopSpin 1.2b and evaluated with XWIN NMR 3.1 or TopSpin 1.2b. All experiments were done at 287.2 K if not otherwise stated. At this temperature, decomposition of AdoMet was not observed, contrary to a temperature of 298 K. The temperature was determined before every experiment with a sample of 4% methanol in methanol-d_4 (*24*).

Resonance assignment was done with HSQC and HMBC spectra at 286.2 K and concentrations of 2 mM AdoMet and 0.01 mM DSS in 1× PBS in D_2O and COSY spectra at 287.1 K and 4 mM AdoMet in the same buffer. Proton spectra were referenced via the DSS signal (0 ppm) or the methyl group of ethanol (1.173 ppm) and in the indirect dimension via the Ξ-scale (factor for ^{13}C: 0.251 449 53).

For STD measurements, we applied a pulse sequence similar to the original one (*20*) but with some modifications of the phase cycle (see figure given in the Supporting Information). In previous experiments, we found a breakthrough of ethanol, methanol, and 1,4-dioxane signals which were presumably caused by nonoptimal subtraction via the phase cycle, especially in the case of leftover magnetization during accumulation of the sequence. The two orthogonal spin locks (2.5 and 5 ms at 10 dB attenuation) were inserted to remove any leftover transverse magnetization at the beginning of the pulse sequence. The subsequent gradient pulse (3 ms, 22 G/cm) has the same cleaning purpose. The selective irradiation therefore starts with a safely prepared spin system. The on- and off-resonance spectrum (complete phase cycles), recorded in an interleafed manner, were stored separately and subtracted afterward. Irradiation of the protein was achieved by a train of selective 90° pulses (50 ms). On-resonance irradiation was done at 0.7 ppm and off-resonance irradiation at 35.7 ppm. After a hard 90° pulse, an additional spin lock pulse (30 ms, 10 dB attenuation) was applied to suppress protein resonances. Typically, we recorded 1K scans per irradiation frequency.

Saturation of the protein during temperature measurements was also tested at 0, 4, and 5.3 ppm.

The STD amplification factor was calculated according to the following equation:

$$A(\mathrm{STD}) = \frac{I_{\mathrm{off}} - I_{\mathrm{on}}}{I_{\mathrm{off}}}$$

where I_{off} and I_{on} are the integral value in the off- and on-resonance spectrum, respectively.

STD buildup curves were recorded by variation of the saturation time, but the total recovery time was kept constant (5 s). For saturation times shorter that 0.5 s, we performed at least two measurements and the individual buildup curves with error bars are given in the Supporting Information. The STD buildup curves were fitted to a polynomial function (second order), and the STD amplification factors for different saturation times were calculated from these functions.

Table 1: T_1 Relaxation Times of 4 mM AdoMet in 1× PBS in D_2O in the Absence of SU(VAR)3−9 or the Presence of 5 μM Su(VAR)3−9

	T_1 (s)	
proton	5 μM SU(VAR)3−9	no SU(VAR)3−9
H_8	2.12	2.04
H_2	5.38	4.19
$H_{1'}$	2.43	2.42
$H_{2'}$	1.92	1.96
$H_{3'}/H_{4'}$	1.34	1.33
$H_{5'}$	0.52	0.51
$H_{5''}$	0.50	0.48
H_α	1.89	1.33
H_β	0.57	0.53
$H_{\gamma'}$	0.54	0.52
$H_{\gamma''}$	1.31	1.39
$(-)SCH_3$	0.94	0.92
$(+)SCH_3$	0.91	0.90

Protons were added to the ligand and the protein in the crystal structure (PDB, 1N6A and 1PEG) with HyperChem, and then the distances (r) of the ligand protons to non-exchangeable protein protons were measured. Only distances up to 5 Å were considered for estimation of the STD factors by the following equation:

$$A(\mathrm{STD})_{\mathrm{theor}} = \frac{1}{r_i^6} + \frac{1}{r_j^6} + \frac{1}{r_k^6} + \ldots$$

T_1 relaxation times were measured with the inversion recovery method. Presaturation on the water signal was applied before the 180° pulse.

RESULTS

Chemical Shift Assignment. Although the chemical shifts of AdoMet are already published (*23*, *25*), we determined these values again because there are several deviations between these publications. Another point was the different conditions (pH, temperature) we used for our measurements. The results of the resonance assignment are shown in the table of the Supporting Information which we obtained using HSQC, HMBC, and COSY methods. After the first submission of this paper, we became aware of a very recent publication where the proton spectra of AdoMet were used for the analysis of dietary supplements (*26*). The reported assignments are in full agreement with ours.

Relaxation Measurements. During titration experiments (not shown), we also determined, for every concentration, the T_1 relaxation times (Table 1) of the ligand protons in the presence and absence of the protein SU(VAR)3−9. At low concentrations, we have not determined the T_1 values of all resonances. Nevertheless, the T_1 values of the ligand protons are relatively constant for different concentrations and independent of the presence or absence of SU(VAR)3−9. One remarkable exception is the adenine proton H_2, where the T_1 values in the presence of the protein are around 1 s longer than they are in the absence of the protein (for every ligand concentration).

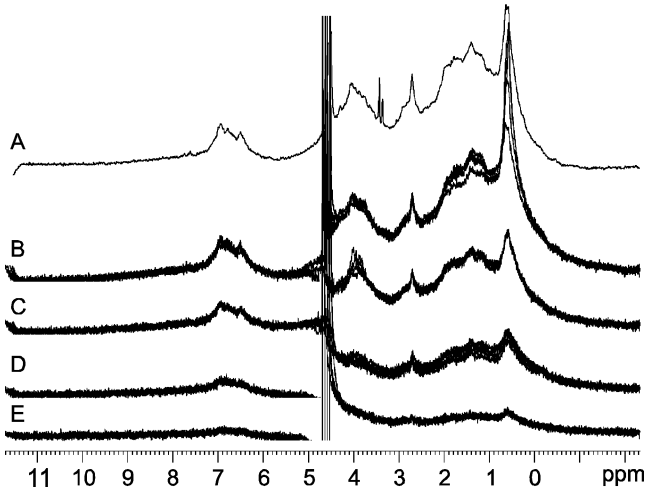

FIGURE 1: STD spectra without protein suppression of 10 μM SU(VAR)3−9*GST and without ligand, in 2× PBS and in D_2O. (A) ^1H control spectra with presaturation recorded at 292.4 K. (B−E) The SU(VAR)3−9*GST protein was irradiated at 0.7 ppm (B), 4 ppm (C), 0 ppm (D), and 5.3 ppm (E) at different temperatures (276.8, 281.8, 287.1, and 292.4 K overlaid for each frequency). The highest degree of saturation is achieved by irradiation at 0.7 ppm and seems to be temperature independent.

Irradiation Site. To ensure complete irradiation of the protein, different irradiation frequencies were tested (Figure 1) with the fusion protein SU(VAR)3−9*GST. We felt it safe to use the less-precious fusion protein for these tests, since only the protein saturation and not the binding was investigated. The irradiation site was tested at four different temperatures because Yan et al. (*27*) found an influence of the temperature for STD measurements.

Irradiation at the methyl groups yields the highest degree of saturation, independent of the temperature (Figure 1B). There seems to be a small temperature dependence for an irradiation frequency of 0 ppm (Figure 1D) as described in ref *27*.

STD-NMR. For the STD-NMR measurements a high ligand excess was used for better STD effects (*20*). Figure 2 shows the STD spectra of 5 μM protein (Figure 2A) and 4 mM AdoMet (Figure 2B). In a solution of 5 μM SU(VAR)3−9 and 4 mM AdoMet (Figure 2C), only resonances of the ligand can be seen. Also the SCH_3 group of the (+)-diastereomer of AdoMet gives no signal in the STD spectrum. The water signal is also present but in opposite phase to the ligand resonances. During the STD buildup curve, no breakthrough of methanol and ethanol was observed. We therefore exclude a contribution of the CH_2 group of ethanol to the STD factors of $H_{\gamma''}$.

Figure 3 shows the STD buildup curve. The adenine protons and the methyl group gave better defined curves than, for example, the methylene protons $H_{5'}/H_{5''}$. This might be caused by the higher signal intensity of the singlets in comparison to the multiplets with intensities close to the level of noise (*27*).

We also performed STD experiments with the fusion protein SU(VAR)3−9*GST, but we also found interactions of the hydrolysis products (cleavage at the sulfur atom and/or of the glycosidic bond) of AdoMet present in the ligand sample. This shows the importance of removing affinity tags and using pure protein samples, to avoid wrong answers of the ligand. Presumably, affinity tags containing histidines are prone to unspecific binding with different ligands.

Binding Epitope. The STD amplification factors were calculated from the polynomial regression. The highest STD factor for each saturation time was set to 100% (Table 2). For the binding epitope (Figure 4), only the values for saturation times of 0.5 and 0.8 s were considered, to avoid effects of incomplete spin diffusion within the protein and relaxation of the ligand.

DISCUSSION

Irradiation at the methyl groups yields the highest degree of saturation of the protein. The saturation of SU(VAR)3−9 is independent of the temperature, at least for three irradiation sites. But for saturation at 0 ppm, a temperature effect as described by Yan et al. (*27*) might be present. Possibly, this effect is also present at the other irradiation sites but not detected because of much lower protein concentration in comparison to the concentration specified in ref *27* and the molecular weight of the fusion protein SU(VAR)3−9*GST (76.2 kDa).

A further aspect of using lower temperature was the decomposition of AdoMet. It is known to be very labile,

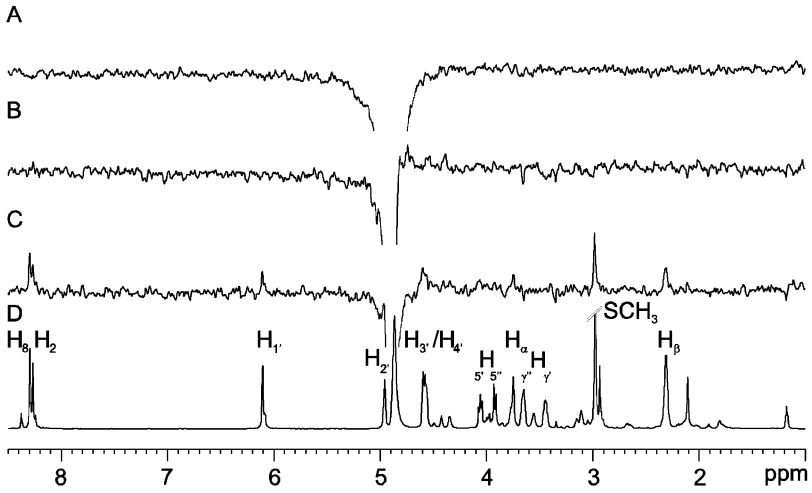

FIGURE 2: STD spectra of (A) 5 μM SU(VAR)3−9 in 1× PBS, (B) 4 mM AdoMet in 1× PBS, and (C) 4 mM AdoMet in the presence of 5 μM SU(VAR)3−9. (D) A normal ^1H control spectrum of the solution in B is shown. In the STD spectrum shown in C, only resonances of the ligand are present.

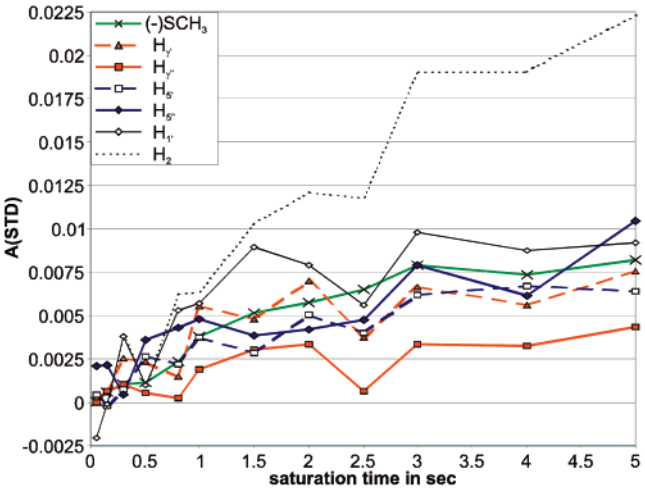

FIGURE 3: STD buildup curve of H_2, the anomeric proton, the methyl group, and the diastereotopic protons $H_{5'}/H_{5''}$ and $H_{\gamma'}/H_{\gamma''}$, respectively. The measurements were performed with 5 μM SU(VAR)3−9 and 2 mM AdoMet in 1× PBS.

Table 2: Comparison of Relative STD Amplification Factors Calculated for Different Saturation Times and Normalized Theoretical STD Intensities[a]

	saturation time			
proton	0.5 s	0.8 s	2 s	$A(STD)_{theor}$
H_8	91	96	91	99
H_2	94	100	100	56
$H_{1'}$	91	94	74[b]	32
$H_{2'}$	nd[c]	nd[c]	nd[c]	nd[d]
$H_{3'}/H_{4'}$	nd[c]	nd[c]	nd[c]	nd[d]
$H_{5'}$	40	42	41	19/96
$H_{5''}$	100	82	nd[e]	
H_α	42	45	47	4
H_β	88	91	78	100[f]
$H_{\gamma'}$	61	65	60	37/45
$H_{\gamma''}$	36	39	40	
$(-)SCH_3$	50	53	52	52[f]

[a] The measurements were performed with 5 mM SU(VAR)3−9 and 2 mM AdoMet in 1× PBS. [b] The STD plateau is reached. [c] Not determined (nd) due to resonance overlap with the water signal. [d] Not determined (nd). [e] Not determined (nd). At longer saturation times the deviation for the measured values is large. [f] Normalized for the number of protons.

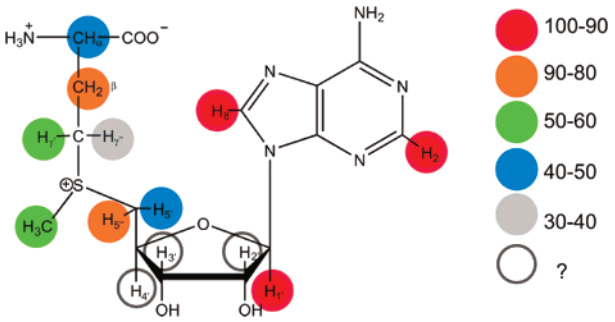

FIGURE 4: Binding epitope of AdoMet to SU(VAR)3−9 (values from Table 2). The adenine protons, $H_{1'}$, $H_{5''}$, and H_β are in close contact with the protein. The $H_{5'}$, the methyl group, H_α, and $H_{\gamma'}$ are in a medium distance to the protein. The $H_{\gamma''}$ has the largest distance to the protein. Because of signal overlap with the water signal, the protons $H_{2'}$, $H_{3'}$, and $H_{4'}$ were not considered. A chemical shift difference of the H_β protons was not observed.

especially under alkaline conditions (*28*). When low concentrations and a pH in the range 4−7 are used, AdoMet is stable for at least several hours (*25*). Under the conditions

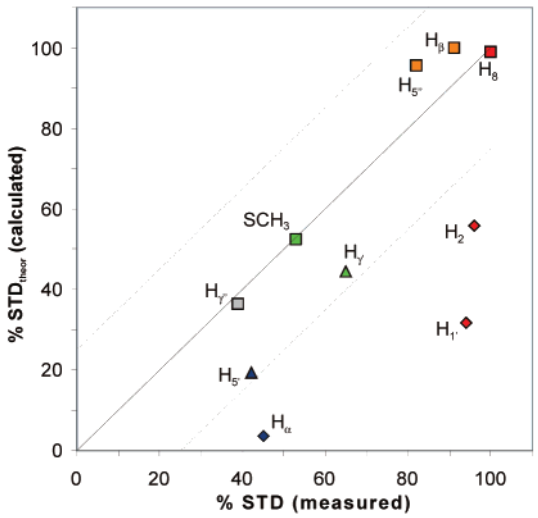

FIGURE 5: Correlation of STD factors and normalized, expected STD_{theor} intensities calculated from the ligand−protein distances. The solid line represents the diagonal, whereas the dashed lines correspond to an interval of ±25%. Squares represent values within ±15%, and triangles represent values within ±25%. Color coding as in Figure 4. For the diastereotopic protons $H_{5'}/H_{5''}$ and $H_{\gamma'}/H_{\gamma''}$, the individual assignments with the better fit were chosen.

we used (pH* 7.8), hydrolysis at 298 K was observable but could be neglected at 287.2 K.

A first result of our experiments is the detection of a binding interaction of AdoMet and SU(VAR)3−9 in solution with STD-NMR. Because of the limitation of the STD method to dissociation constants in the range 10^{-3}−10^{-8} M, we can also conclude that the K_D of the investigated interaction has to be in this range (K_D values given for SET7/9 and SET7/9 mutants are about 10 μM (*14*)). The resonance corresponding to the methyl group of the (+)-diastereomer shows no STD signal and therefore does not bind to SU(VAR)3−9. Our main intention was to determine the binding epitope of AdoMet to SU(VAR)3−9. To exclude T_1 relaxation effects (*27*), we used only short saturation times for epitope mapping. There seems to be no disturbance of the epitope map by T_1 relaxation (at least for the saturation times considered) because H_β with a T_1 value of around 0.5 s has a very high STD factor, comparable to the adenine protons with much larger T_1 times. Similarly, the diastereotopic H_5 protons show different STD amplification values despite the same T_1 relaxation times.

Five protons out of 10 are in good agreement with our binding epitope of AdoMet and the crystal structure of SET7/9. Furthermore, two protons are within ±25% (Figure 5) of the expected STD values.

Our results show a close contact of the adenine moiety to the protein. This is in good agreement with the crystal structure (*13*) (Figure 6, PDB 1N6A and 1N6C), where this aromatic ring is enclosed by the protein. Nevertheless, the measured STD intensity for H_2 is double the value expected (Table 2). This might be due to differences in the amino acid sequence between SET7/9 and SU(VAR)3−9 (Trp-352 in SET7/9 is not present in SU(VAR)3−9). Interestingly, this proton has also the highest T_1 value, which is increased by around 1 s in the presence of only 5 μM SU(VAR)3−9. We attribute these different T_1 values of H_2 in the presence and absence of SU(VAR)3−9 to the anticonformation of the glycosidic bond in the crystal structure. In NOE spectra (not

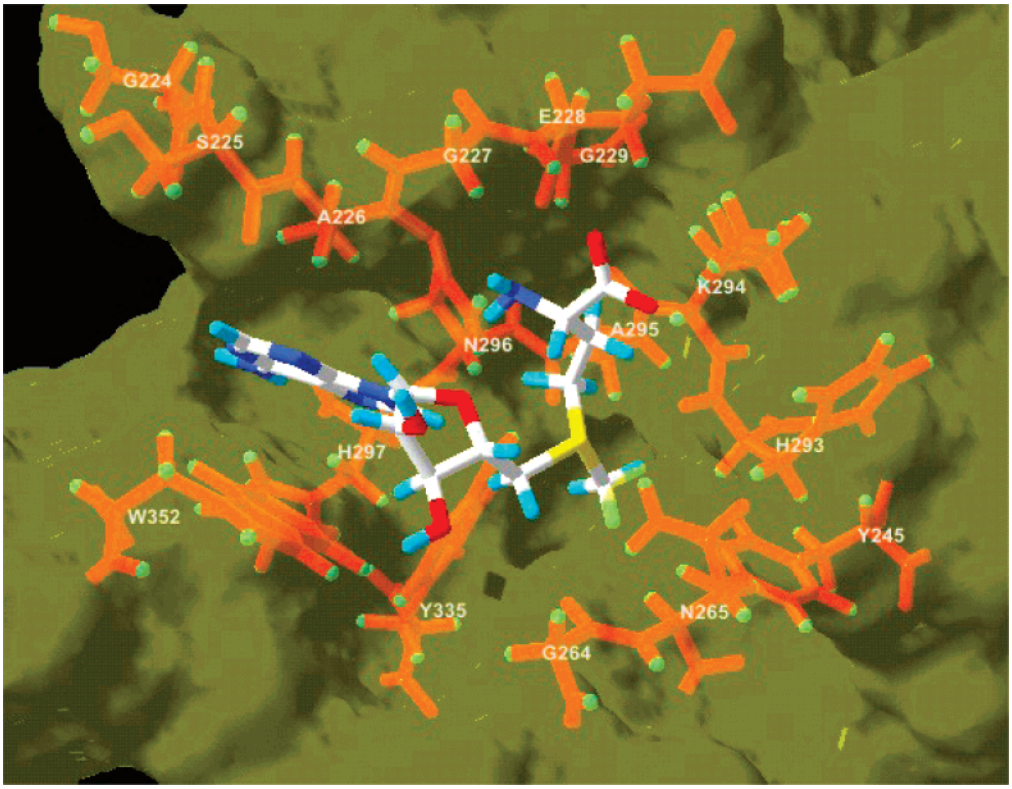

FIGURE 6: *S*-adenosyl-L-methionine bound to SET7/9 (taken from the crystal structure (*13*), PDB 1N6A). Our STD measurements favor a similar binding epitope for AdoMet to SU(VAR)3−9. The picture was generated with DeepView/Swiss-PdbViewer v3.7.

shown), we observe contacts between H_8 and the sugar part as described in ref *29*. H_2 shows only a few weak NOE contacts and has therefore less possibilities for cross relaxation, which is reflected in the longest relaxation time observed. In presence of the protein, the cross relaxation seems to be further diminished, most likely due to a fixed anticonformation in the bound state.

The anomeric proton and the two H_β protons show also high STD factors, reflecting close contacts to the protein, but this can only be seen in the crystal structure for H_β. Further agreement can be observed for the methyl group with medium range STD factors. The higher distance of the methyl group to the protein is biochemically reasonable because this group points toward the channel through which the lysine side chain enters the active site. H_α shows also a medium range STD factor, but from the crystal structure, no STD contact is expected.

The diasterotopic methylene protons $H_{5'}/H_{5''}$ and $H_{\gamma'}/H_{\gamma''}$ show high STD factors for one and low STD factors for the other proton. This is not unexpected but not in total agreement with the X-ray structure. One explanation is again a difference in the amino acid sequence and a different conformation of SU(VAR)3−9 in solution compared to SET7/9 in the crystal state. Recently, the conformation in the crystal structure of UDP-galactose bound to galactosyltransferase, which was not compatible to the STD results, was refined using STD intensity restraints (*30*). The resulting structure was in accordance with the STD-NMR results. In addition, we observe dynamic processes in solution with NMR which are not reflected by X-ray results. The main reason might be differences in the amino acid sequence of the AdoMet binding pocket of SET7/9 and SU(VAR)3−9. Although this sequence is conserved, some deviations are present. Ala-295 in SET7/9 is in the vicinity of $H_{\gamma'}/H_{\gamma''}$. The corresponding residue in SU(VAR)3−9 is Ile-559. These additional atoms might be responsible for a conformational change in the amino acid moiety of AdoMet.

Our data indicate a possibility to determine the absolute configuration of these diastereotopic protons because only one combination of experimental and calculated STD factors is in agreement, with clear differences for $H_{5'}/H_{5''}$ and minor ones for $H_{\gamma'}/H_{\gamma''}$.

Our STD experiments favor a similar structure of the AdoMet binding pocket of SU(VAR)3−9 in solution in comparison to SET7/9. This demonstrates the power of STD measurements in such cases.

In an additional approach suggested by a referee, the measured STD factors were compared with the STD factors derived from the crystal structure of DIM-5 with bound AdoHcy and histone peptide (*31*, PDB entry 1PEG). The correlation of the STD factors shows no coincidence for most of the protons (data not shown).

This might be due to a different amino acid composition of the binding pocket compared to SET7/9 (alignment scheme in the Supporting Information) and/or due to the ligand itself (AdoHcy might show different interactions with the protein than AdoMet). Furthermore, the crystal structure of DIM-5 (*31*) has a large binding pocket for AdoHcy, whereas the binding pocket of AdoMet in SET7/9 (*13*) clasps around the adenine moiety of AdoMet. There might be a structural change of the c-SET helix upon binding of AdoMet leading to further contact between the SET7/9 and AdoMet.

CONCLUSIONS

STD-NMR measurements were used to investigate the binding interactions of *S*-adenosyl-L-methionine to SU-

(VAR)3−9. It was shown that AdoMet binds to SU-(VAR)3−9 in a similar manner as shown by X-ray crystallography for SET7/9. The adenine protons, the anomeric proton, H_{β}, and $H_{5''}$ are in close contact to the protein. The methyl group which is transferred to the ϵ-amino group of lysine has an average distance of 2.5 Å to the nearest protein protons. It appears that the structure of the binding pocket is very similar in the crystal state and in solution. The binding epitope will lead to further investigation of SU(VAR)3−9 mutants with different activity. We plan to combine STD measurements with the transfer NOE technique to test possible conformational changes of the ligand. We will also perform investigations with the cofactor product *S*-adenosyl-L-homocysteine. The (+)-diastereomer of AdoMet does not bind to SU(VAR)3−9.

ACKNOWLEDGMENT

The authors thank Claudia Peikert for helpful discussions and Dr. Bermel (Bruker Biospin) for helpful discussions and modifying the pulse sequence.

SUPPORTING INFORMATION AVAILABLE

Tables showing the assignment of AdoMet resonances (Table 1), the sequence alignment of the SET-domain in SU-(VAR)3−9, SET7/9, and DIM-5 (Table 2), and the calculated distances from AdoMet protons to protons of nearest amino acids in SU(VAR)3−9 (Table 3) and figures showing the pulse sequence for the 1D-STD-NMR measurements (Figure 1), the individual STD buildup curves (Figure 2), the binding pocket of AdoMet within SU(VAR)3−9 (Figure 3), and the binding pocket of AdoHcy in DIM-5 (Figure 4). This material is available free of charge via the Internet at http://pubs.acs.org.

REFERENCES

1. Michal, G., Ed., (1999) *Biochemical Pathways. 1.*, Spektrum Akademischer Verlag, Heidelberg, Germany.
2. Blackburn, G. M., Gamblin, S. J., and Wilson, J. R. (2003) Mechanism and control in biological amine methylation, *Helv. Chim. Acta 86*, 4000−4006.
3. Turner, B. M. (2000) Histone acetylation and an epigenetic code, *BioEssays 22*, 836−845.
4. Strahl, B. D., and Allis, C. D. (2000) The language of covalent histone modifications, *Nature 403*, 41−45.
5. Jenuwein, T., and Allis, C. D. (2001) Translating the histone code, *Science 293*, 1074−1080.
6. Czermin, B., Schotta, G., Hulsmann, B. B., Brehm, A., Becker, P. B., Reuter, G., and Imhof, A. (2001) Physical and functional association of SU(VAR)3−9 and HDAC1 in *Drosophila*, *EMBO Rep.* 2, 915−919.
7. Schotta, G., Ebert, A., Krauss, V., Fischer, A., Hoffmann, J., Rea, S., Jenuwein, T., and Reuter, G. (2002) Central role of *Drosophila* SU(VAR)3−9 in histone H3-K9 methylation and heterochromatic gene silencing, *EMBO J. 21*, 1121−1131.
8. Nakayama, J., Rice, J. D., Strahl, B. D., Allis, C. D., and Grewal, S. I. S. (2001) Role of histone H3 lysine 9 methylation in epigenetic control of heterochromatin assembly, *Science 292*, 110−113.
9. Tamaru, H., and Selker, E. U. (2001) A histone H3 methyltransferase controls DNA methylation in *Neurospora crassa*, *Nature 414*, 277−283.
10. Rea, S., Eisenhaber, F., O'Carroll, D., Stahl, B. D., Sun, Z.-W., Schmid, M., Opravil, S., Mechtler, K., Ponting, C. P., Allis, C. D., and Jenuwein, T. (2000) Regulation of chromatin structure by site-specific histone H3 methyltransferases, *Nature 406*, 593−599.
11. Ebert, A., Schotta, G., Lein, S., Kubicek, S., Krauss, V., Jenuwein, T., and Reuter, G. (2004) Su(var) genes regulate the balance between euchromatin and heterochromatin in *Drosophila*, *Genes Dev. 18*, 2973−2983.
12. Jacobs, S. A., Harp, J. M., Devarakonda, S., Kim, Y., Rastinejad, F., and Khorasanizadeh, S. (2002) The active site of the SET7/9 domain is constructed on a knot, *Nat. Struct. Biol. 9*, 833−838.
13. Kwon, T., Chang, J. H., Kwak, E., Lee, C. W., Joachimiak, A., Kim, Y. C., Lee, J. W., and Cho, Y. (2003) Mechanism of histone lysine methyl transfer revealed by the structure of SET7/9-AdoMet, *EMBO J. 22*, 292−303.
14. Wilson, J. R., Jing, C., Walker, P. A., Martin, S. R., Howell, S. A., Blackburn, M. G., Gamblin, S. J., and Xiao, B. (2002) Crystal structure and functional analysis of the histone methyltransferase SET7/9, *Cell 111*, 105−115.
15. Xiao, B., Jing, C., Wilson, J. R., Walker, P. A., Vasisht, N., Kelly, G., Howell, S., Taylor, I. A., Blackburn, G. M., and Gamblin, S. J. (2003) Structure and catalytic mechanism of the human histone methyltransferase SET7/9, *Nature 421*, 652−656.
16. Zhang, X., Tamaru, H., Khan, S. I., Horton, J. R., Keefe, L. J., Selker, E. U., and Cheng, X. (2002) Structure of the *Neurospora* SET domain protein DIM-5, a histone H3 lysine methyltransferase, *Cell 111*, 117−127.
17. Trievel, R. C., Beach, B. M., Dirk, L. M. A., Houtz, L, and Hurley, J. H. (2002) Structure and catalytic mechanism of a SET domain protein methyltransferase, *Cell 111*, 91−103.
18. Min, J., Zhang, X., Cheng, X., Grewal, S. I. S., and Xu, R.-M. (2002) Structure of the SET domain histone lysine methyltransferase Clr4, *Nat. Struct. Biol. 9*, 828−832.
19. Mayer, M., and Meyer, B. (1999) Charakterisierung von Ligandenbindung durch Sättigungstransfer-Differenz-NMR-Spektroskopie, *Angew. Chem. 111*, 1902−1906.
20. Mayer, M., and Meyer, B. (2001) Group epitope mapping by saturation transfer difference NMR to identify segments of a ligand in direct contact with a protein receptor, *J. Am. Chem. Soc. 123*, 6108−6117.
21. Meyer, B., and Peters, T. (2003) NMR-Techniken zum Screening und zur Identifizierung der Bindung von Liganden an Proteinrezeptoren, *Angew. Chem. 115*, 890−918.
22. Shiozaki, S., Kawasaki, K., Kanagawa, J. P., Yamada, H., Tani, Y., Shimizu, S., and Kyoto, J. P., (1984) Procedure for the purification of *S*-Adenosyl-L-methionine, *Ger. Offen.* 3329218.
23. Schalk-Hihi, C., and Markham, G. D. (1999) The conformations of a substrate and product bound to the active site of *S*-adenosylmethionine synthetase, *Biochemistry 38*, 2542−2550.
24. Berger, S., and Braun, S. (2004) *200 and More NMR Experiments*, pp 141−144, VCH Verlag, Leipzig, Germany.
25. Stolowitz, M. L., and Minch, M. J. (1981) *S*-Adenosyl-L-methionine and *S*-adenosyl-L-homocysteine, an NMR study, *J. Am. Chem. Soc. 103*, 6015−6019.
26. Hanna, G. M. (2004) NMR regulatory analysis: determination and characterization of *S*-adenosyl-L-methionine in dietary supplements, *Pharmazie 59*, 251−256.
27. Yan, J., Kline, A. D., Mo, H., Shapiro, M. J., and Zartler, E. R. (2003) The effect of relaxation on the epitope mapping by saturation transfer difference NMR, *J. Magn. Reson. 163*, 270−276.
28. Borchardt, R. T. (1979) Mechanism of alkaline hydrolysis of *S*-adenosyl-L-methionine and related sulfonium nucleosides, *J. Am. Chem. Soc. 101*, 458−463.
29. Markham, G. D., Norrby, P.-O., and Bock, C. W. (2002) *S*-Adenosylmethionine conformations in solution and in protein complexes: conformational influence of the sulfonium group, *Biochemistry 41*, 7636−7646.
30. Jayalakshmi, V., Biet, T., Peters, T., and Krishna, N. R. (2004) Refinement of the conformation of UDP-galactose bound to galactosyltransferase using the STD-NMR intensity-restrained CORCEMA optimization, *J. Am. Chem. Soc. 126*, 8610−8611.
31. Zhang, X., Yang, Z., Khan, S. I., Horton, J. R., Tamaru, H. Selker, E. U., and Cheng, X. (2003) Structural basis for the product specificity of histone lysine methyltransferases, *Mol. Cell 12*, 177−185.

BI047749X